



Original article

Quercetin prevents myocardial infarction adverse remodeling in rats by attenuating TGF- β 1/Smad3 signaling: Different mechanisms of action

Ghadeer M. Albadrani ^{a,*}, Mona N. BinMowyna ^b, May N. Bin-Jumah ^a, Gehan El-Akabawy ^{c,d}, Hussain Aldera ^e, Ammar M. AL-Farga ^f

^a Department of Biology, College of Science, Princess Nourah Bint Abdulrahman University, Riyadh, Saudi Arabia

^b College of Applied Medical Sciences, Shaqra University, Shaqra, Saudi Arabia

^c Department of Basic Sciences, College of Medicine, Princess Nourah Bint Abdulrahman University, Riyadh, Saudi Arabia

^d Department of Anatomy and Embryology, Faculty of Medicine, Menoufia University, Menoufia, Egypt

^e Department of Basic Medical Sciences, College of Medicine, King Saud bin Abdulaziz University for Health Sciences (KSAU-HS), Riyadh, Saudi Arabia

^f Biochemistry Department, College of Sciences, University of Jeddah, Jeddah, Saudi Arabia



ARTICLE INFO

Article history:

Received 15 December 2020

Revised 19 January 2021

Accepted 1 February 2021

Available online 13 February 2021

Keywords:

Quercetin
Heart
Remodeling
Fibrosis
TGF- β 1
BMPs
Smad
Rats

ABSTRACT

This study investigated the anti-remodeling and anti-fibrotic and effect of quercetin (QUR) in the remote non-infarcted of rats after myocardial infarction (MI). Rats were divided as control, control + QUR, MI, and MI + QUR. MI was introduced to the rats by ligating the left anterior descending (LAD) coronary artery. All treatments were given for 30 days, daily. QUR persevered the LV hemodynamic parameters and prevented remote myocardium damage and fibrosis. Also, QUR suppressed the generation of ROS, increased the nuclear levels of Nrf2, and enhanced SOD and GSH levels in the LVs of the control and MI model rats. It also reduced angiotensin II, nuclear level/activity of the nuclear factor NF- κ B p65, and protein expression of TGF- β 1, α -SMA, and total/phospho-smad3 in the LVs of both groups. Concomitantly, QUR upregulated LV smad7 and BMP7. In conclusion, QUR prevents MI-induced LV remodeling by antioxidant, anti-inflammatory, and anti-fibrotic effects mediated by ROS scavenging, suppressing NF- κ B, and stimulating Nrf-2, Smad7, and BMP7.

© 2021 The Author(s). Published by Elsevier B.V. on behalf of King Saud University. This is an open access article under the CC BY-NC-ND license (<http://creativecommons.org/licenses/by-nc-nd/4.0/>).

1. Introduction

Adverse cardiac remodeling and fibrosis are common pathological mechanisms that alter the geometry and function of the left ventricles (LVs) after myocardial infarction (MI) (Ma et al., 2018; Hanna and Frangogiannis, 2019). While fibrosis prevents damage in the infarcted area, it compromises the LV function in the viable myocardium and eventually leads to heart failure (HF) (Sun, 2009; Reichert et al., 2016). In the heart, the transforming growth factor- β (TGF- β) superfamily plays significant roles in regulating numerous biological functions including cell differentiation, proliferation,

survival, and fibrosis (Hanna and Frangogiannis, 2019). Among all, TGF- β 1, released from cardiomyocytes, inflammatory cells, activated fibroblast, and lymphocytes, is the most commonly studied factor that is correlated with cardiac fibrosis, hypertrophy, and apoptosis in the viable myocardium after injury or infarction (Schneiders et al., 2005; Huntgeburth et al., 2011; Edgley et al., 2012; Khan et al., 2016).

Increased expression of TGF- β 1 was reported in the infarcted, border, and remote areas of the LV after MI (Dobaczewski et al., 2011; Saxena et al., 2014; Hanna and Frangogiannis, 2019). However, the cellular effects of TGF β 1 on the target cells involve both canonical (Smad-dependent) and non-canonical (e.g. p38 MAPK, TAK1, RhoA, and ERK) pathways (Liu et al., 2016). Currently, it is well accepted that the canonical ALK5/Smad2/3 pathway is the major pathway that mediates the fibrotic and apoptotic effects of TGF- β 1 in the survival myocardium by inducing fibroblast activation, inhibiting proteases (i.e. Matrix metalloproteinases (MMPs) and collagenases), upregulating MMPs protease inhibitors, and stimulating the release of the connective tissue growth factor (CTGF) (Leask and Abraham, 2004; Mauviel, 2005; Schneiders

* Corresponding author at: P.O. Box 84428, Riyadh 11671, Saudi Arabia.

E-mail address: gmalbadrani@pnu.edu.sa (G.M. Albadrani).

Peer review under responsibility of King Saud University.



Production and hosting by Elsevier

et al., 2005; Liu et al., 2016; Ma et al., 2018). Yet, the bone morphogenetic protein7 (BMP7) and Smad7 are natural anti-fibrotic and anti-apoptotic which can inhibit the cardiac smad2/3 signaling (Wu et al., 2014; Sanders et al., 2016).

Modern cardiology encourages the search for cheaper and safer drugs from natural resources such as polyphenols and flavonols (Zhang et al., 2018; Ferenczyova et al., 2020). Quercetin (QR) is a common flavonol that is widely found in numerous fruits and vegetables (Shu et al., 2017; Ferenczyova et al., 2020). QR has well reported cardioprotective effects and demonstrated *in vitro* and *in vivo* in several animal models including doxorubicin (DOX), isoproterenol, angiotensin II (ANG II), aldosterone, salt, high fructose-diet, Duchenne muscular dystrophy, and autoimmune myocarditis-induced cardiac damage (Ferenczyova et al., 2020). Besides, the cardioprotective effect of QR was demonstrated in animal models of MI and ischemia/reperfusion (I/R)-induced injury where it effectively reduces the size of the infarction, stimulated cardiomyocytes survival, and improved LV function (Liu et al., 2016; Tang et al., 2019). All these beneficial effects of QR were attributed to its antioxidant, anti-inflammatory, and anti-apoptotic effects (Ferenczyova et al., 2020).

Recently, the anti-fibrotic cardio-protective effect of QR was demonstrated in the failing hearts of rats after isoproterenol or ANGII treatment mediated by downregulation/inhibiting TGF- β 1 (Li et al., 2013; Wang et al., 2020). Besides, QR prevented high-fat diet (HFD)-induced cardiac remodeling and fibrosis by inhibiting the nuclear factor kappa-beat (NF- κ β) and activating the nuclear factor erythroid 2-related factor 2 (Nrf2), two master inflammatory and antioxidant transcription factors, respectively (Panchal et al., 2012).

Despite these findings, the anti-fibrotic effect of QR on the cardiac remodeling of the survival myocardium of animals after induction of MI is still unclear. Therefore, this study was designed to investigate this effect by targeting the precise mechanism of action including its effects on key pathways such as ANG II release, TGF- β 1/Smad3/7 signaling, activities of Nrf2, and NF- κ B p65, and the expression of BMP2/7.

2. Materials and methods

2.1. Drugs, chemicals, antibodies, and reagents

Quercetin (QR) (Cat# Q4951) and Carboxymethyl Cellulose (CMC) (Cat# C5678-500G) were purchased from Sigma Aldrich (St. Louis, MO, USA). Colorimetric and ELISA kits to measure levels of Troponin-I (Cat# E4737), creatinine kinase-MB (CKMB) (Cat# E4608), interleukin-6 (Cat# K4145), superoxide dismutase (SOD) (Cat# E458), tumor necrosis factor- α (TNF- α) (Cat# K1052), reduced glutathione (GSH) (Cat. NO. K454), and malondialdehyde (MDA) (Cat# K454) were purchased from BioVision, CA, USA. ROS assay kit (Cat# E-BC-K138-F) was purchased from Elabscience, CA, USA. A recombinant NF- κ B p65 protein (Cat# 31102) and ELISA kit to measure the nuclear activity of NF- κ B p65 (Cat# 40096) were purchased from Active Motif, Tokyo, Japan. An ELISA kit to measure serum and tissue levels of ANG II (Cat# CSB-E04494r) was purchased from CUSABIO, TX, USA. ANG II cocktail inhibitor (Cat# 9000681) was purchased from Cayman Chemicals, USA.

2.2. Antibodies

Antibodies against Nrf2 (Cat# 12712), NF- κ B p65 (Cat# 3034), collagen A1 (Cat# 66948), collagen 3A (Cat#30565), alpha-smooth muscle actin (α -SMA) (Cat#19245), β -actin (Cat# 4970), and Lamin A (Cat# 86846) were purchased from Cell Signalling, USA. Antibodies against TGF β -1 (Cat# sc-130348), smad3 (Cat#

sc-101154), smad7 (Cat# sc-365846), phospho-smad3 (Ser⁴²⁵) (Cat# sc-517575), and BMP7 (Cat# sc-53917) were purchased from Santa Cruze biotechnology, USA. A Bradford-based protein assay kit (Cat# 23200), phosphate buffer saline solution (Cat# 20012043), protease inhibitor cocktail (Cat# A32965), radio-immuno-precipitation assay RIPA buffer (RIPA) buffer (Cat# ab156-34); and nuclear-cytoplasmic/nuclear extraction kit (Cat# 78833) were purchased from ThermoFisher scientific.

2.3. Animals and ethics

Adult health Wistar albino male rats (140 \pm 15 g) from the α breed were kindly provided with care from the Experimental Animal Care Center at King Saud University, Riyadh, Saudi Arabia. All rats were housed in separate plastic cages (5/cage) under 12/12 h (dark/light), 21 \pm 2 $^{\circ}$ C, and 53–63% humidity. All rats had a full access to their normal chow and water all through the experimental period. All procedures included in this study were approved by the Institutional Review Board (IRB. No: 20-0177), Princess Nourah Bint Abdulrahman University, Riyadh, Saudi Arabia.

2.4. Induction of MI

The induction of MI was introduced to the rats by ligating the LAD coronary artery as previously described by Eid et al. (2020). In brief, each rat was anesthetized using 1.9 mg/kg ketamine/xy-lazine hydrochloride solution. Once anesthesia was confirmed, a gel was placed on the rat's eyes and the rat was placed on a heating blanket and the temperature was recorded by an anal probe. Then, the rat were placed on a small animal ventilator and artificially ventilated. The chest was opened over by cutting ribs 2 and 4 and the heart was exposed. The pericardium was removed and the LAD coronary artery was ligated using 6/0 sutures. The chest was then closed in three layers and the rats was returned to its cage and monitored over the next 2 days.

2.5. Experimental design

Rats were classified into 5 groups (n = 12/group) in the following order: 1) Control sham-operated group: had a similar sham surgical procure without tying the left anterior descending (LAD) coronary artery and then received an equivalent oral dose of 0.5% carboxymethyl cellulose (CMC) (a vehicle), daily, for the next 30 days; 2) Control + QR treated group: had similar sham surgery as in group but then received QR (prepared in 0.5% CMC) (50 mg/kg/orally) for 30 days; 3) MI-induced group: were rats with pre-established MI and received 0.5% CMC as a vehicle for the next 30 days starting 1 h after the induction of MI, and 4) MI + QR-treated group: were rats with pre-established MI and administered QR solution, 1 h post-induction of MI (50 mg/kg/orally) and continued for the next 30 days starting. The preparation, dose, and route of administration of this QR were adopted from previous studies, which demonstrated cardioprotective and anti-fibrotic effects of QR at this dose (Zaafan et al., 2013; Bin-Jalialh, 2017; Wang et al., 2020).

2.6. Recording of the hemodynamic parameter

By the end of day 30 and over 3 days, the rats were anesthetized by 60 mg/kg of 1% sodium pentobarbital solution, i.p. LV function was studied using a Millar catheter and a Powerlab system (Model ML780, ADInstruments, Australia) and analyzed using LabChart 8 (ADInstruments, Australia) as previously described by Eid et al. (2020). The measured hemodynamic parameters were 1) LVSP: LV systolic pressure, 2) dP/dt_{max}: maximum derivative of the change in systolic pressure over time, 3) dP/dt_{min}: minimum

derivative of the change in diastolic pressure; and 4) LVEDP: LV end-diastolic pressure.

2.7. Serum collection and biochemical measurement in the serum

Serum samples were collected after the hemodynamic parameters. Accordingly, 2 ml of blood were withdrawn from the carotid artery into plain gel-containing tubes. Some other samples (0.5 ml) were collected in plain tubes containing ANG II inhibitors for the analysis of ANG II. All blood samples were centrifuged (10 min/1500 × g/room temperature) to collect sera. All samples were kept at -20°C and then used to measure the levels of CK-MB, ANG II, and Troponin-I levels using the provided kits.

2.8. Tissue collection and preparation

The rats were ethically killed by the cervical dislocation protocol. The hearts were removed on ice. The infarcted area was identified by the pale color. The remote non-infarcted myocardial (and corresponding area in the other non-infarcted groups) were extracted and cut into smaller pieces. Parts of these LVs were directly snap-frozen in liquid nitrogen, kept at -70°C . Other parts of the LVs were placed in 10% buffered formalin.

2.9. Tissue fractionation, preparation, and cardiac biochemical measurements

In some parts, the nuclear/cytoplasmic fractions were prepared using the provided kit. Both fractions were stored at -80°C until used. The activities of NF- κB p65 in the nuclear fractions of all samples were determined using the provided kit and standard. Other parts of each LV (40 mg) were homogenized in 9 volumes ml ice-cold PBS, centrifuged at 11000g at 4°C for 15 min to collect the total cell homogenates. These were stored at -80°C and used later for the biochemical analysis to measure the levels of TNF α , IL-6, SOD, GSH, MDA, ROS, and ANG II, using the above-mentioned provided kits. However, for the analysis of ANGII, the tissue was homogenized in the presence of 10 μL ANG II inhibitor. Also, other parts of the frozen LVs (30 mg) were homogenized in 0.25 ml RIPA buffer plus 10 μL protease inhibitor and centrifuged as above. The resulted homogenates were then stored at -80°C and used later for western blotting. Protein concentration in all samples was determined using the provided Bradford-based protein assay kit. All biochemical analyses were performed for 6 rats for each group and as per the manufacturers' instructions.

2.10. Western blotting

Proteins collected from the total cell homogenates and nuclear fraction were loaded in 1x loading dye (2 $\mu\text{g}/\mu\text{l}$) and boiled for 5 min. Then, a total of 40 μg proteins were loaded and separated by SDS-PAGE (various ratios/6–12%) and transferred to nitrocellulose membranes. Each membrane was then incubated with the target 1st antibody (2 h/room temperature/rotation) followed by a second incubation with the 2nd antibody. The developed reactions were detected using the provided enhanced Chemiluminescence detergent. Band intensities were evaluated by the C-Di Git blot scanner (LI-COR, NE, USA). A single membrane was stripped up to 3 times and phosphorylated forms were detected first. The relative expression of the nuclear proteins was normalized with the corresponding expression of lamin A whereas the relative expression of total proteins was normalized with the corresponding expression of β -actin.

2.11. Histological evaluation

Freshly collected parts of the LV of the remote myocardium were fixed in 10% buffered formalin. LVs samples were then dehydrated in increasing alcohol concentrations and exposed to xylene clearance. The tissues were then embedded in paraffin, sectioned (3–5 μm), and routinely stained with either hematoxylin and eosin (for morphological analysis) or Masson's trichrome (MT) stain (for fibrosis evaluation). All pictures were collected under a light microscope by a blind investigator.

2.12. Statistical analysis

GraphPad Prism software (version 8) was used to analyze the data. The analysis was performed using -way ANOVA and Tukey's post hoc test. Data were considered significantly varied at $p < 0.05$. Average readings were presented as mean \pm SD.

3. Results

3.1. QUR prevents the MI-induced increase in hearts weight and circulatory levels of cardiac enzymes and serum levels of ANG II

Heart weights and serum levels of CK-MB, troponin I, and ANG II were not significantly changed between the control (sham-operated) and control + QUR-treated rats but were significantly increased in the MI-induced rats as compared to both groups (Fig. 1A–D). However, the heart weights and serum levels of all these markers were significantly decreased in the MI + QUR-treated rats as compared to MI-induced rats (Fig. 1A–D).

3.2. QUR preserves cardiac function and structure in infarcted rats and increases contractility in the control hearts

The levels of LVSP showed a significant increase in control + QUR-treated rats as compared to control rats (Fig. 2A–D). However, higher levels of LVEDP with a concomitant reduction in the values of LVSP, dp/dt_{min} , and the dp/dt_{max} were observed in the MI-induced rats as compared to the control rats (Fig. 2A–D). On the other hand, the administration of QUR to MI-induced rats (MI + QUR) reversed the alterations in all these hemodynamic parameters as compared to MI-induced rats (Fig. 2A–D).

3.3. QUR preserves the structure of the LVs of the control rats and the remote myocardium of the infarcted hearts

Viable myocardia of the LVs of the control and control + QUR showed intact cardiomyocytes and myofibrils structures and abundant intercalated disks (Fig. 3A&B). On the other hand, abnormally oriented, damaged, and hypertrophied muscle fibers with nuclear fading (karyolysis) and increased infiltration of inflammatory cells were observed in the remote myocardia of the LVs of MI-induced rats (Fig. 3C&D). However, almost normally appeared muscle fibers with a reduction in cardiomyocyte size (hypertrophy) and inflammatory cell infiltration, intact nuclei structure, and reduced myofibrils damage were observed in the LVs of MI + QUR-treated rats (Fig. 3E&F).

3.4. QUR inhibits inflammation in remote myocardium of MI-induced rats but suppresses ROS, NF- κB , and ANG II and boosts antioxidants levels in the remote myocardium of both the control and MI-induced hearts

Levels of TNF- α and IL-6 were not significantly different but the nuclear activity and protein levels of NF- κB p65, as well as the

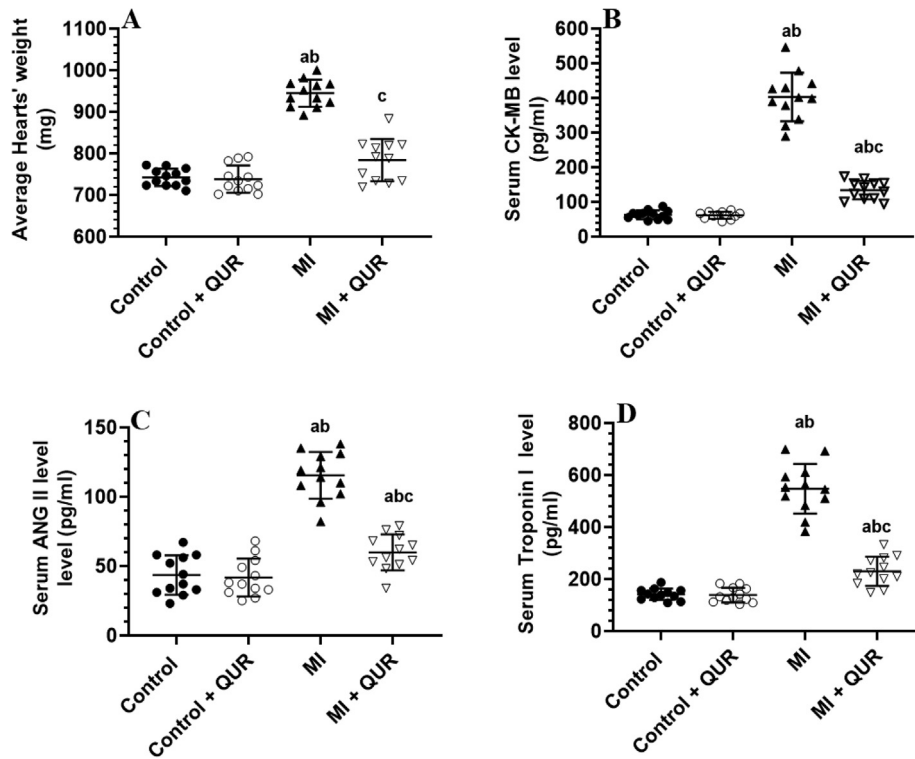


Fig. 1. Average heart weights (A) and serum levels of creatinine kinase-MB (B), angiotensin II (ANG II) (C), and Troponin-1 (D) in all groups of rats. Data are expressed as mean \pm SD of 12 rats/groups. ^a: significantly different as compared to control rats, ^b: significantly different as compared to control + Quercetin (QUR)-treated rats; and ^c: significantly different as compared with the myocardial infarction (MI)-induced rats.

levels of ANG II, have significantly decreased in the viable myocardia of the LVs of control + QUR-treated rats as compared to sham-

operated control rats (Fig. 4A-E). Concomitantly, levels of MDA were not changed but the levels of ROS were significantly

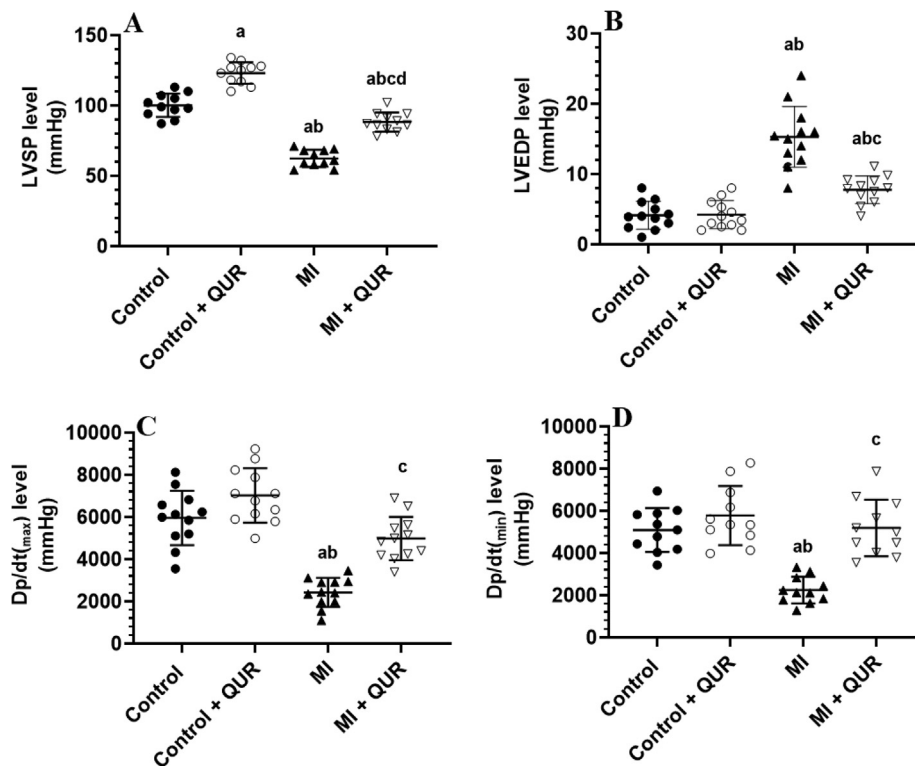


Fig. 2. Cardiac hemodynamic function in the hearts of all groups of rats. Data are expressed as mean \pm SD of 12 rats/groups. ^a: significantly different as compared to control rats, ^b: significantly different as compared to control + Quercetin (QUR)-treated rats; and ^c: significantly different as compared with the myocardial infarction (MI)-induced rats. LVEDP: LV end-diastolic pressure. LVSP: LV systolic pressure.

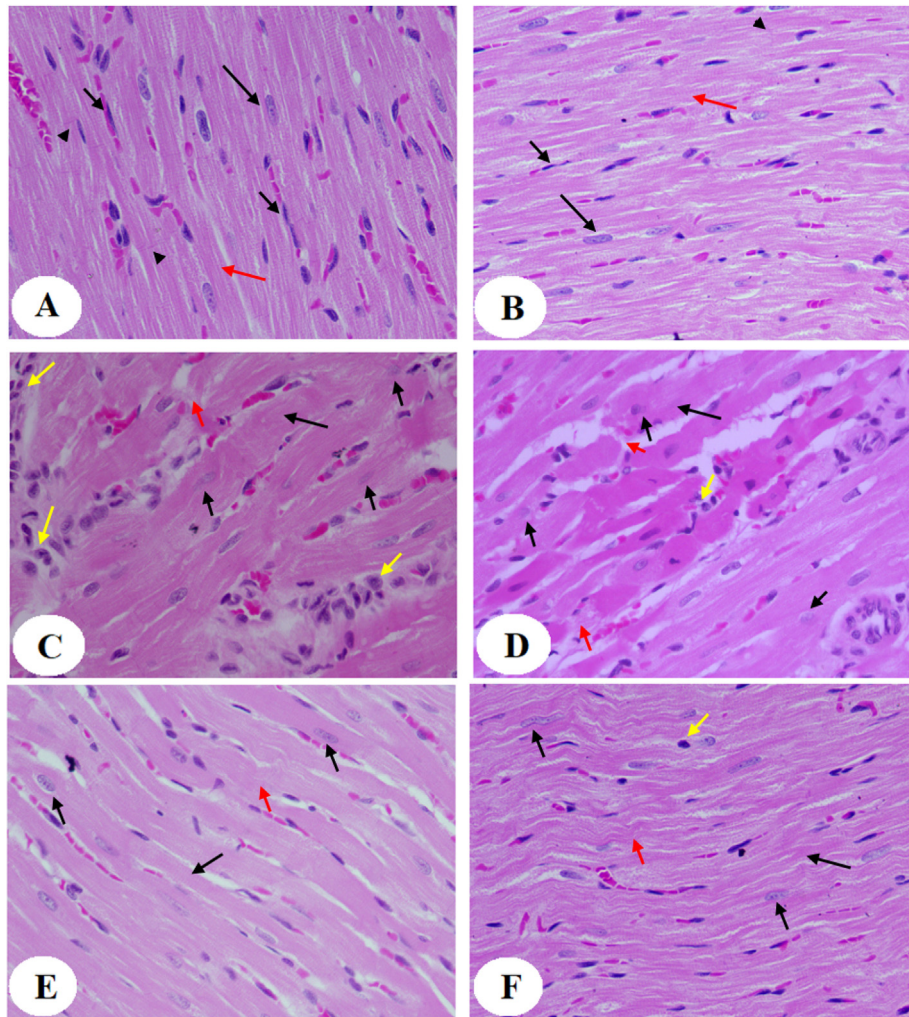


Fig. 3. Photomicrographs of the non-infarcted left ventricles (LVs) of all groups of rats. (200X). **A and B:** were taken from corresponding areas of the LVs of the control (sham-operated) and control + Quercetin (QR)-treated rats and showed intact muscle fibers (red arrow), intercalated disk (arrowhead), cardiomyocytes nuclei (long black arrow) and endothelial nuclei (short black arrow). **C & D:** were taken from the remote myocardia of the LVs of myocardial infarcted (MI)-induced rats and showed abnormalities in the organization of myofibrils, hypertrophied muscle fibers (long black arrow), damaged muscle fibers (red arrow), infiltration of inflammatory cells (yellow arrow), and nuclear fading (Karyolysis) (short black arrow). **E and F:** were taken from the remote myocardia of the LVs of MI+ treated rats and showed much improvement in the structure and orientation of the myofibrils (long black arrow), as well as a normal size of the myofibrils (red arrow). Also, the endothelial and cardiomyocytes nuclei appeared normal (short black arrow). However, few infiltrating cells were still observed (yellow arrow) with no obvious cardiomyocytes damage.

decreased and levels of SOD, and GSH, as well as the total protein levels of Nrf-2, were significantly increased in the LVs of control + QR-treated rats as compared to sham-operated control rats (Fig. 5A-E). On the other hand, levels of MDA, ROS, ANG II, TNF- α , and IL-6, as well the nuclear activity and protein levels of NF- κ B p65 were significantly increased but the levels of SOD, GSH, and total protein levels of Nrf-2 were significantly decreased in the remote myocardia of MI-induced rats as compared to control sham-operated rats (Fig. 4A-E and Fig. 5A-E). The alteration in the levels of all these biochemical endpoints was significantly reversed in the remote myocardia of the LVs of MI + QR as compared to MI-induced rats (Fig. 4A-E and Fig. 5A-E).

3.5. QR prevents collagen synthesis and deposition in the remote myocardia of the LVs of MI-induced rats

The amount of collagen deposited in the viable LVs and the protein levels of collagen 1A and 3A were not significantly different between the control and control + QR-treated rats but were significantly increased in the remote myocardia of the LVs of the MI-induced rats as compared to both groups (Fig. 6A-G). Adminis-

tration of QR to MI-induced rats (MI + QR) significantly lowered the expression of both collagen 1A and 3A and reduced the amount of collagen deposition in the remote myocardia of their LVs as compared to MI-induced rats (Fig. 6A-G).

3.6. QR downregulates TGF- β 1 and Smad3, inhibits Smad3 phosphorylation (activation), and upregulates BMP7 and Smad7 in the remote myocardia of both the control and MI-induced rats

Total protein levels of TGF- β 1, Smad3, p-smad3 (Ser425), and α -SMA were significantly increased but total protein levels of Smad7 and BMP7 were significantly downregulated in the remote myocardia of MI-induced rats as compared to sham-operated control rats (Fig. 7A-C and Fig. 8A&B). Total levels of Smad3 were not significantly different between the control and control + QR-treated rats (Fig. 7C). Nevertheless, the protein levels of TGF- β 1, α -SMA, and p-smad3 (Ser⁴²⁵) were significantly suppressed but protein levels of Smad7 and BMP7 were significantly upregulated in the remote myocardia/LVs of both the control + QR and MI + QR-treated rats as compared sham-operated and MI-induced rats, respectively (Fig. 7A-C and Fig. 8A&B).

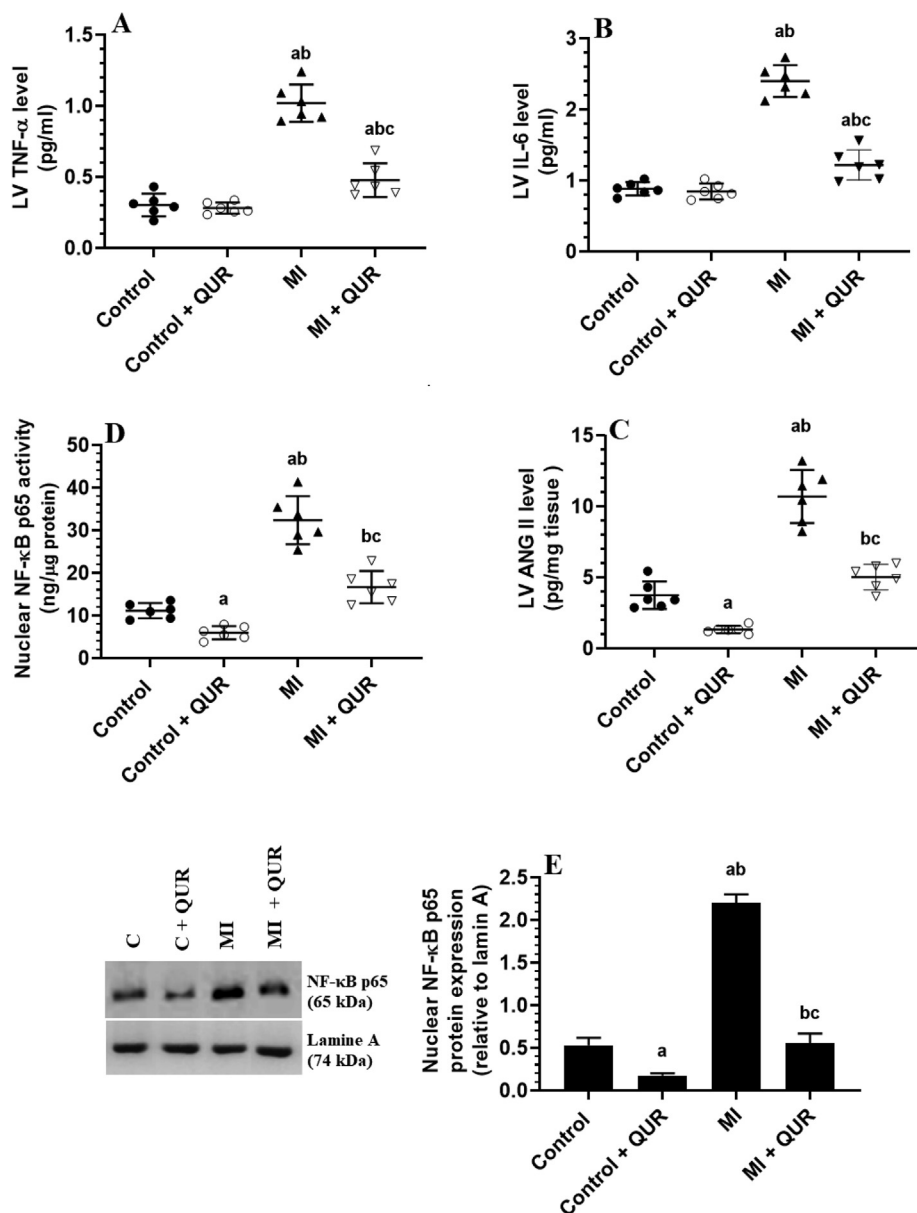


Fig. 4. Levels of tumor necrosis factor (TNF- α) (A), interleukin-6 (IL-6) (C), and angiotensin II (ANG II) (C), as well as the nuclear activity (D) and levels (E) of NF- κ B in the viable non-infarcted myocardia of the left ventricles (LVs) of all groups of rats. Data are expressed as mean \pm SD of 6 rats/groups. ^a: significantly different as compared to control rats, ^b: significantly different as compared to control + Quercetin (QUR)-treated rats; and ^c: significantly different as compared with the myocardial infarction (MI)-induced rats.

4. Discussion

This study identified novel protective and anti-fibrotic effects of QUR in the viable remote myocardium of rats, 4 weeks after induction MI. The major finding showed that QUR was able to blunt fibroblast activation and collagen synthesis through downregulating and suppressing TGF- β 1/Smad-3 signaling, associated with 1) reducing cardiac levels of ANG II, 2) scavenging ROS through increasing antioxidants and the expression of Nrf-2/HO-1, 3) suppressing inflammation by inhibiting NF- κ B and the production of the inflammatory cytokines, and 4) activation of Smad7 and upregulation of BMP2/7.

Dysregulated deposition of ECM (i.e. collagen) in the viable myocardium induces pathological regenerative fibrosis that impairs LV function and ultimately ends with HF (Nguyen et al., 2010; Reichert et al., 2016). The first observations in this study that

confirm the anti-hypertrophic and anti-fibrotic effects of QUR in the LVs of the MI-induced rat, was the obvious improvement in all measured hemodynamic parameter and LV histological feature. Besides, further evidence is derived from the ability of QUR to prevent the increase in heart weights, serum levels of CKMB and Troponin I, and the expression and deposition of collagen in the remote myocardium of the infarcted hearts of these rats. Supporting our data, subacute administration of QUR (25 mg – 50 50 mg/kg) attenuated LV hypertrophy, improved LV structure, increased ejection fraction (EF), and suppressed collagen deposition in the viable myocardia of different animal's models including isoproterenol; ANG II, aldosterone, and HFD-induced cardiac fibrosis (Shahbaz et al., 2011; Panchal et al., 2012; Li et al., 2013).

However, the TGF- β 1/Smad2/3 is the major fibrotic signaling pathway in the viable myocardium during the late stages post-MI (Dobaczewski et al., 2011; Ma et al., 2018). While the ANG II

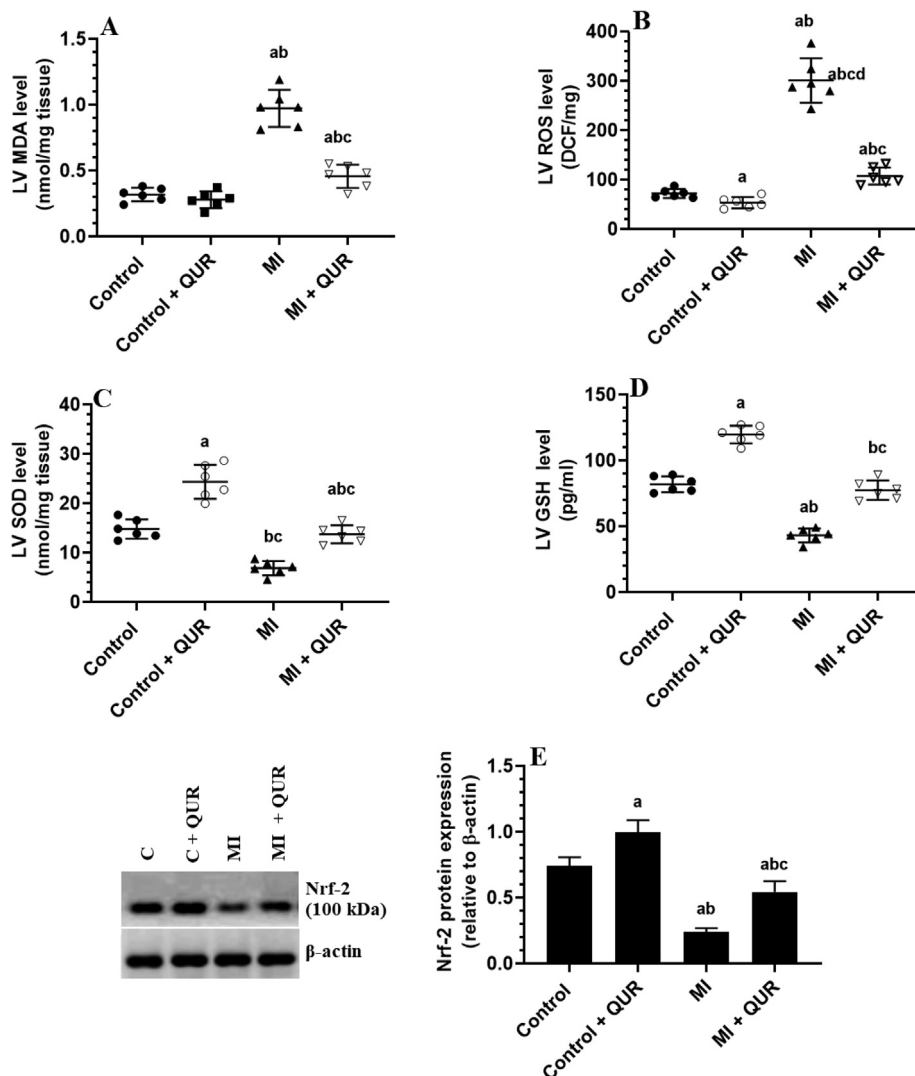


Fig. 5. Levels of reactive oxygen species (ROS), malondialdehyde (MDA) (B), superoxide dismutase (SOD) (C), and reduced glutathione (GSH) (D), as well protein levels of the nuclear factor erythroid 2-related factor 2 (Nrf-2) (E) in the viable non-infarcted myocardia of the left ventricles (LVs) of all groups of rats. Data are expressed as mean \pm SD of 6 rats/groups. ^a: significantly different as compared to control rats, ^b: significantly different as compared to control + Quercetin (QUR)-treated rats; and ^c: significantly different as compared with the myocardial infarction (MI)-induced rats.

and pressure overload induces the activation smad2 pathway in the heart of experimental animals, smad3 is most commonly activated in the non-infarcted myocardium post-MI (Chen et al., 2014; Lal et al., 2014; Guo et al., 2015). In this study, the anti-fibrotic effect of QUR in the remote myocardium of rats involved downregulation of TGF- β 1, reduced phosphorylation of smad3 (inhibition), and decreasing fibroblast activation (low α -SMA expression).

Of note, ANGII, ROS, NF- κ B p65 and inflammatory cytokines are the best activators of TGF β 1 in the infarcted and non-infarcted myocardium (Spinale, 2007; Frangogiannis, 2012; Moris et al., 2017; Liu et al., 2018). However, the promoter region of TGF- β 1 lacks an NF- κ B p65 binding site (Perez et al., 1994), suggesting that ROS and increasing inflammatory cytokines released from the cardiac cells or infiltrating macrophages are the major triggers for TGF- β 1 activation (Onai et al., 2007). Interestingly, Smad7 is a potent anti-fibrotic and anti-inflammatory protein in most cardiac cells that inhibit TGF- β 1/smard2/3 and NF- κ B p65 (Wei et al., 2013; Ma et al., 2017). Low expression levels of smad7 were reported in the ischemic or failing hearts and were correlated with the severity and degree of the LV fibrosis and remodeling (Wang et al., 2002;

Wei et al., 2013). However, ANG II is reported to be the common inhibitor of Smad7 (Wei et al., 2013).

To understand the possible mechanisms by which QUR suppresses the levels and signaling of TGF- β 1/smard3 in the LVs of MI-induced rats, we have measured the levels of all the above-mentioned fibrotic/anti-fibrotic markers in the LVs of these rats. As expected, we have found a significant reduction in the nuclear levels/activation of NF- κ B p65 that is coincided with reduced levels of ANGII, ROS, MDA, IL-6, and TNF- β 1, and increased levels of SOD and GSH Smad7 in the viable myocardia of MI + QUR-treated rats. Besides, QUR also increased the expression of Nrf-2, master antioxidant transcription factors in most tissues including the heart (Pall and Levine, 2015). With no change in MDA and ROS levels, similar alterations were also seen in the LVs of control rats that were treated with the same concentration of QUR. Accordingly, this suggests that the anti-fibrotic effect of QUR involves suppressing ANG II and inflammatory cytokines, inhibiting NF- κ B p65, scavenging ROS, and stimulating the expression of Smad7 and Nrf-2. It also indicates that the antioxidant potential of QUR is possibly mediated by the upregulation of Nrf2. Since ANG II

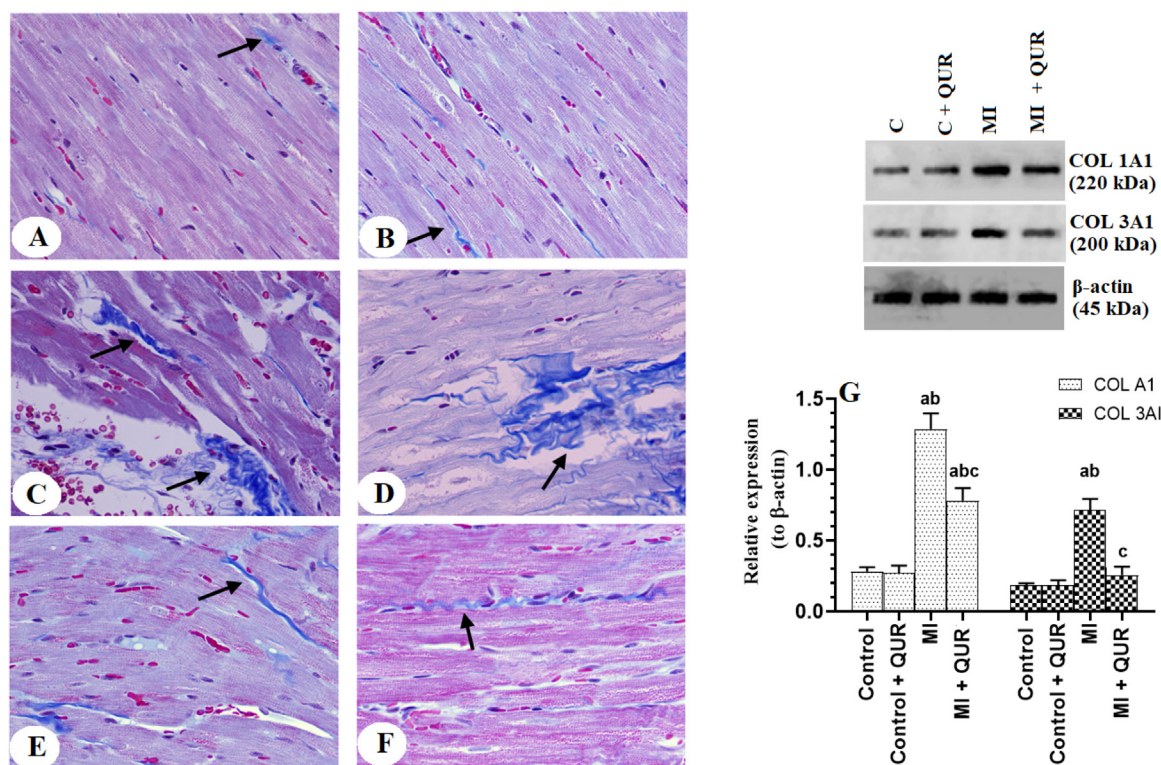


Fig. 6. Photomicrographs of the left ventricles (LVs) of rats from all experimental groups as stained by Masson's trichrome stain (A-F) and protein levels of collagen 1A1 and 3A1 (G) in the viable non-infarcted myocardia of the LVs of all groups of rats. Collagen deposition is indicated by the blue color. **A and B:** were taken from the corresponding LVs sham-operated (control) and control + QUR-treated rats. **C and D:** were taken from the remote myocardia myocardial infarcted (MI) hearts. **E and F:** were taken from the remote myocardia of MI + QUR-treated rats. In G: data are expressed as mean \pm SD of 6 rats/groups. ^a: significantly different as compared to control rats; ^b: significantly different as compared to control + Quercetin (QUR)-treated rats; and ^c: significantly different as compared with the myocardial infarction (MI)-induced rats.

downregulates Smad-7, our data may suggest that the stimulatory effect of QUR on Smad7 could be secondary to reducing cardiac production of ANG II or reducing cardiac peripheral ANG II stimulation, which could be also predicted from the previously reported decrease in serum levels of ANG II in the control and MI + QUR-treated rats.

Nonetheless, previous reports have shown that ROS rapidly activates NF- κ B in ischemic hearts (Moris et al., 2017). The anti-inflammatory potential of QUR is well reported in several studies (Miles et al., 2014; D'Andrea, 2015; Ferenczyova et al., 2020). Besides, QUR can inhibit cardiac NF- κ B p65 in the hearts of I/R hearts activating the peroxisome proliferator-activated receptor (PPAR) (Liu et al., 2016). Also, QUR can directly prevent the cardiac transcription of NF- κ B in rats exposed to sodium nitrate-induced myopathy and I/R injury (Liu et al., 2016; Fadda et al., 2018). Furthermore, QUR suppresses inflammation in other tissue by decreasing the production of inflammatory prostaglandins through inhibiting cyclo-oxygenase 1 (COX1) and lipoxygenase-12 (12-LOX) enzymes, which mediate the arachidonic acid metabolism (O'Leary et al., 2004; Takano-Ishikawa et al., 2006). In addition to these mechanisms and the given the contradictory effect of ROS and Smad7 on the activity of NF- κ B p65, we could also assume that the anti-inflammatory effect of QUR occurs indirectly due to its antioxidant potential and its ability to activate smad7, possibly directly or through attenuating ANG II levels. This can't be confirmed based on our data and further studies are required to confirm this.

Besides, QUR can suppress the cardiac synthesis of ANG II animal models of hypertension and HF. Within this view, QUR sup-

pressed LV fibrosis and reduced serum levels of ANG II and aldosterone in isoproterenol-treated rats (Li et al., 2013). However, the mechanism by which QUR inhibits ANG II production remained elusive based on our data. This could be due to cardiac or systemic effects mediated by inhibiting ACE and/or downregulating AT1 receptors as previously demonstrated in hypertensive animals (Häckl et al., 2002; Lesjak et al., 2018). Concerning its antioxidant potential, QUR also prevented the adverse remodeling in the LVs of DOX and HFD-fed rats by increasing the levels of endogenous antioxidant enzymes and GSH and upregulating/activation of Nrf-2/heme-oxygenase-1 (HO-1) axis (Panchal et al., 2012). Also, QUR can increase the intracellular GSH levels directly by activation of γ -glutamylcysteine synthase (GCS), a critical enzyme that stimulates GSH synthesis (Li et al., 2016). Besides, QUR has a potent ROS scavenging potential due to the presence of 5-OH (hydroxyl) groups on its backbone (Lesjak et al., 2018).

Nonetheless, similar to the effect afforded by smad7, BMP7 is another important anti-fibrotic and anti-inflammatory mediator in mammalian hearts (Hanna and Frangogiannis, 2019). Another interesting finding in this study is the higher expression of BMP7 in the heart of the control and MI-induced rats, which received QUR. In the heart, BMP7 can suppress fibrosis by inhibiting the TGF β 1/smad2/3 signaling and the endothelial to mesenchymal transition (Merino et al., 2016). Exogenous administration of BMP7 attenuated the decline in cardiac function and prevented cardiac remodeling of infarcted hearts (Jin et al., 2018). Also, BMP7 inhibits cardiac inflammation by promoting the polarization of M2 macrophages (Urbina and Singla, 2014). Therefore, we could strongly argue that the anti-fibrotic effect of QUR is mediated by

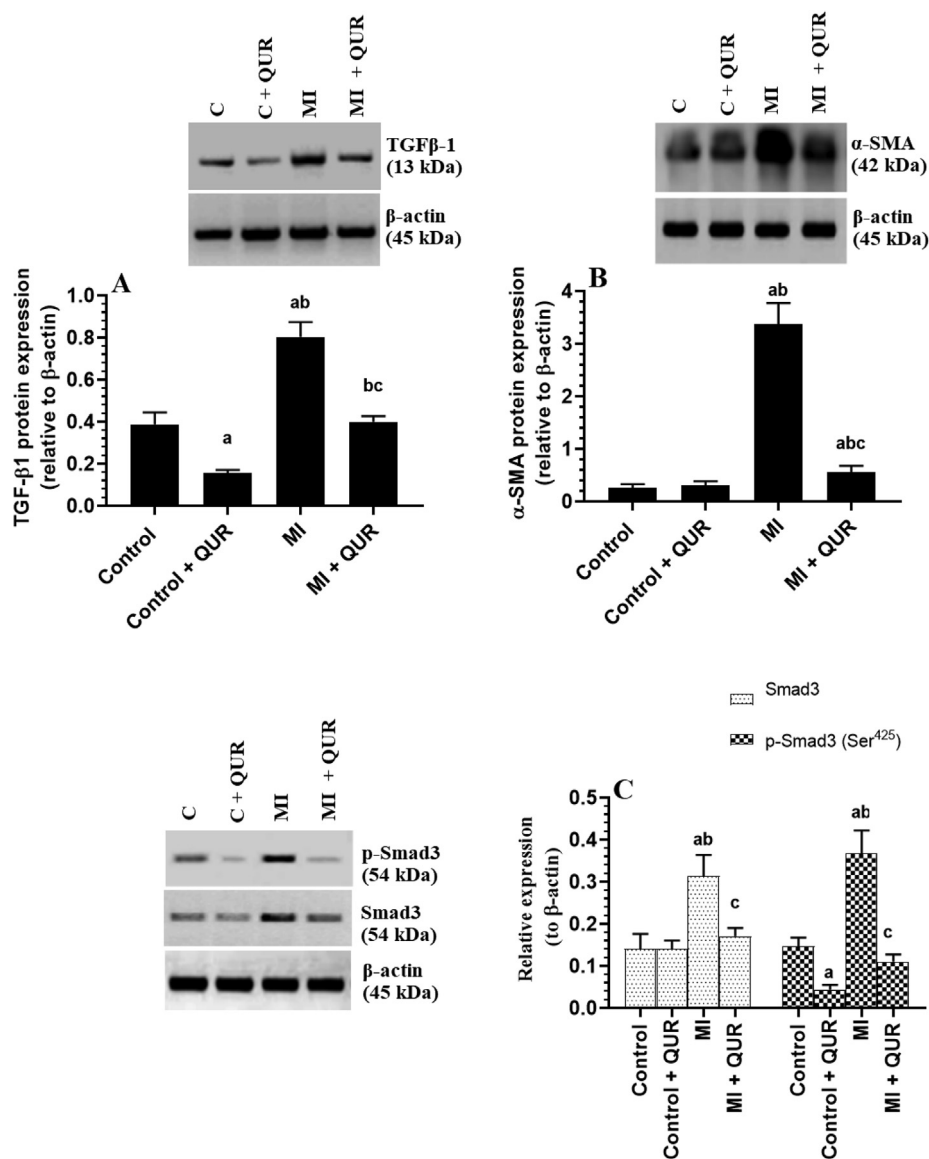


Fig. 7. Protein levels of transforming growth factor-β1 (TGF-β1) (A), smooth muscle actin-α (B), and total and phosphorylated Smad-3 (Ser⁴²⁵) (C) in the viable non-infarcted myocardia of the left ventricles (LVs) of all groups of rats. Data are expressed as mean ± SD of 6 rats/groups. ^a: significantly different as compared to control rats, ^b: significantly different as compared to control + Quercetin (QUR)-treated rats; and ^c: significantly different as compared with the myocardial infarction (MI)-induced rats.

the independent upregulation of MBP7. This finding is novel and the first to show such an effect, which further adds more mechanism for its anti-inflammatory and anti-fibrotic effects of QUR. Supporting these findings, kaempferol, another similar flavonoid, also inhibited renal fibrosis by upregulation of BMP7-induced activation of smad1/5 signaling. Despite these findings, this study may still have some limitations. For example, in this study, we have targeted the effect of QUR on the remote non-infarcted myocardium of MI-rats. Such protective effect could be also due to the initial protective effect of QUR on the infarct myocardium. Therefore, further studies investigated all these mechanisms should be also performed in the infarcted area. Also, the data reported in this study still observational which is another limitation of this study. Therefore, further studies using animals deficient with major key players such as AT1, smad7, BMP7 should be used in future research to confirm these findings.

In conclusion, the findings of this study confirm a potent protective effect of QUR against MI-induced cardiac remodeling that hap-

pens after MI. These data are encouraging for further well-organized clinical trials in a trail to discover new safe therapeutics.

Declaration of Competing Interest

The authors declare that they have no known competing financial interests or personal relationships that could have appeared to influence the work reported in this paper.

Acknowledgment

The authors would like to thank the Deanship of Scientific Research at Princess Nourah bint Abdulrahman University, Riyadh, Saudi Arabia, through the Research Funding Program (Grant No# FRP-1442-18) for the funding this study.

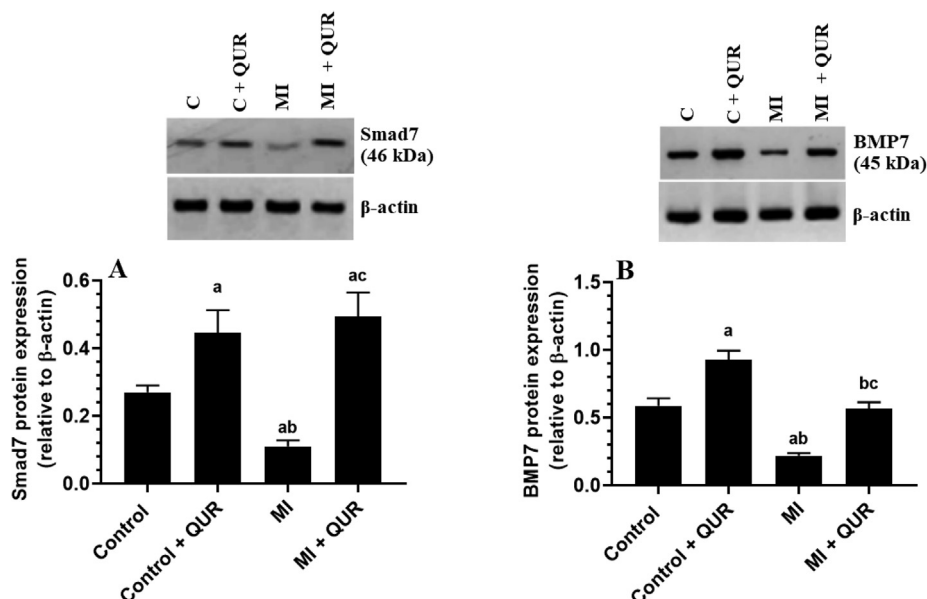


Fig. 8. Total protein levels of Smad7 (A) and bone morphogenetic protein-7 (BMP7) (B) in the viable non-infarcted myocardia of the left ventricles (LVs) of all groups of rats. Data are expressed as mean \pm SD of 6 rats/groups. ^a: significantly different as compared to control rats; ^b: significantly different as compared to control + Quercetin (QUR)-treated rats; and ^c: significantly different as compared with the myocardial infarction (MI)-induced rats.

Funding

This research was funded by the Deanship of Scientific Research at Princess Nourah bint Abdulrahman University, Riyadh, Saudi Arabia, through the Research Funding Program (Grant No# FRP-1442-18).

References

- Bin-Jalil, I., 2017. Quercetin inhibits chronic stress-induced myocardial infarction in rats. *Int. J. Morphol.* 35 (4), 1363–1369.
- Chen, Y., Yang, S., Yao, W., Zhu, H., Xu, X., Meng, G., Zhang, W., 2014. Prostacyclin analogue beraprost inhibits cardiac fibroblast proliferation depending on prostacyclin receptor activation through a TGF β -Smad signal pathway. *PLoS ONE* 9, (5) e98483.
- D'Andrea, G., 2015. Quercetin: A flavonol with multifaceted therapeutic applications?. *Fitoterapia* 106, 256–271.
- Dobaczewski, M., Chen, W., Frangogiannis, N.G., 2011. Transforming growth factor (TGF)- β signaling in cardiac remodeling. *J. Mol. Cell. Cardiol.* 51 (4), 600–606.
- Edgley, A.J., Krum, H., Kelly, D.J., 2012. Targeting fibrosis for the treatment of heart failure: a role for transforming growth factor- β . *Cardiovasc. Ther.* 30 (1), e30–e40.
- Eid, R.A., Alharbi, S.A., El-Kott, A.F., Eleawa, S.M., Zaki, M., El-Sayed, F., Eldeen, M.A., Aldera, H., Al-Shudiefat, A., 2020. Exendin-4 ameliorates cardiac remodeling in experimentally induced myocardial infarction in rats by inhibiting PPAR1/NF- κ B axis in a SIRT1-dependent mechanism. *Cardiovasc. Toxicol.* 20 (4), 401–418.
- Fadda, L.M., Attia, H.A., Al-Rasheed, N.M., Ali, H.M., Al-Rasheed, N.M., 2018. Roles of some antioxidants in modulation of cardiac myopathy induced by sodium nitrite via down-regulation of mRNA expression of NF- κ B, Bax, and flt-1 and suppressing DNA damage. *SPJ.* 26 (2), 217–223.
- Ferencyzova, K., Kalocayova, B., Bartekova, M., 2020. Potential implications of quercetin and its derivatives in cardioprotection. *Int. J. Mol. Sci.* 21 (5), 1585.
- Frangogiannis, N.G., 2012. Extracellular matrix proteins in cardiac adaptation and disease. *Physiol. Rev.* 92 (2), 635–688.
- Guo, H., Zhang, X., Cui, Y., Zhou, H., Xu, D., Shan, T., Zhang, F., Guo, Y., Chen, Y., Wu, D., 2015. Taxifolin protects against cardiac hypertrophy and fibrosis during biomechanical stress of pressure overload. *Toxicol. Appl. Pharmacol.* 287 (2), 168–177.
- Häckel, L.P., Cuttle, G., Dovichi, S.S., Lima-Landman, M.T., Nicolau, M., 2002. Inhibition of angiotensin-converting enzyme by quercetin alters the vascular response to bradykinin and angiotensin I. *Pharmacology* 65 (4), 182–186.
- Hanna, A., Frangogiannis, N.G., 2019. The role of the TGF- β superfamily in myocardial infarction. *Front. Cardiovasc. Med.* 6, 140.
- Huntgeburth, M., Tiemann, K., Shahverdyan, R., Schlüter, K. D., Schreckenberg, R., Gross, M. L., Mödersheim, S., Caglayan, E., Müller-Ehmsen, J., Ghanem, A., Vantler, M., Zimmermann, W. H., Böhm, M., Rosenkranz, S., 2011. Transforming

- growth factor β 1 oppositely regulates the hypertrophic and contractile response to β -adrenergic stimulation in the heart. *PLoS one.* 6 (11), e26628.
- Jin, Y., Cheng, X., Lu, J., Li, X., 2018. Exogenous BMP-7 facilitates the recovery of cardiac function after acute myocardial infarction through counteracting TGF- β 1 signaling pathway. *Tohoku J. Exp. Med.* 244 (1), 1–6.
- Khan, S.A., Dong, H., Joyce, J., Sasaki, T., Chu, M.L., Tsuda, T., 2016. Fibulin-2 is essential for angiotensin II-induced myocardial fibrosis mediated by transforming growth factor (TGF)- β . *Lab Invest.* 96 (7), 773–783.
- Lal, H., Ahmad, F., Zhou, J., Yu, J.E., Vagnozzi, R.J., Guo, Y., Yu, D., Tsai, E.J., Woodgett, J., Gao, E., Force, T., 2014. Cardiac fibroblast glycogen synthase kinase-3 β regulates ventricular remodeling and dysfunction in ischemic heart. *Circulation* 130 (5), 419–430.
- Leask, A., Abraham, D.J., 2004. TGF- β signaling and the fibrotic response. *FASEB J.* 18 (7), 816–827.
- Lesjak, M., Beara, I., Simin, N., Pintač, D., Majkić, T., Bekvalac, K., Orčić, D., Mimica-Dukić, N., 2018. Antioxidant and anti-inflammatory activities of quercetin and its derivatives. *J. Funct. Foods.* 40, 68–75.
- Li, M., Jiang, Y., Jing, W., Sun, B., Miao, C., Ren, L., 2013. Quercetin provides greater cardioprotective effect than its glycoside derivative rutin on isoproterenol-induced cardiac fibrosis in the rat. *Can. J. Physiol. Pharmacol.* 91 (11), 951–959.
- Li, Y., Yao, J., Han, C., Yang, J., Chaudhry, M.T., Wang, S., Liu, H., Yin, Y., 2016. Quercetin, inflammation and immunity. *Nutrients* 8 (3), 167.
- Liu, C.L., Guo, J., Zhang, X., Sukhova, G.K., Libby, P., Shi, G.P., 2018. Cysteine protease cathepsins in cardiovascular diseases: from basic research to clinical trials. *Nat. Rev. Cardiol.* 15 (6), 351–370.
- Liu, X., Yu, Z., Huang, X., Gao, Y., Wang, X., Gu, J., Xue, S., 2016. Peroxisome proliferator-activated receptor γ (PPAR γ) mediates the protective effect of quercetin against myocardial ischemia-reperfusion injury via suppressing the NF- κ B pathway. *Am. J. Transl. Res.* 8 (12), 5169–5186.
- Ma, C., Jiang, Y., Zhang, X., Chen, X., Liu, Z., Tian, X., 2018. Isoquercetin ameliorates myocardial infarction through anti-inflammation and anti-apoptosis factor and regulating TLR4-NF- κ B signal pathway. *Mol. Med. Rep.* 17 (5), 6675–6680.
- Ma, Y., Zou, H., Zhu, X.X., Pang, J., Xu, Q., Jin, Q.Y., Ding, Y.H., Zhou, B., Huang, D.S., 2017. Transforming growth factor β : A potential biomarker and therapeutic target of ventricular remodeling. *Oncotarget.* 8 (32), 53780–53790.
- Mauviel, A., 2005. Transforming growth factor- β : a key mediator of fibrosis. *Methods Mol. Med.* 117, 69–80.
- Merino, D., Villar, A.V., García, R., Tramullas, M., Ruiz, L., Ribas, C., Cabezero, S., Nistal, J.F., Hurlé, M.A., 2016. BMP-7 attenuates left ventricular remodeling under pressure overload and facilitates reverse remodeling and functional recovery. *Cardiovasc. Res.* 110 (3), 331–345.
- Miles, S.L., McFarland, M., Niles, R.M., 2014. Molecular and physiological actions of quercetin: need for clinical trials to assess its benefits in human disease. *Nutr. Rev.* 72 (11), 720–734.
- Moris, D., Spartalis, M., Spartalis, E., Karachaliou, G.S., Karaolanis, G.I., Tsourouflis, G., Tsilimigras, D.I., Tzatzaki, E., Theocharis, S., 2017. The role of reactive oxygen species in the pathophysiology of cardiovascular diseases and the clinical significance of myocardial redox. *Ann. Transl. Med.* 5 (16), 326.
- Nguyen, D.T., Ding, C., Wilson, E., Marcus, G.M., Olgin, J.E., 2010. Pirfenidone mitigates left ventricular fibrosis and dysfunction after myocardial infarction and reduces arrhythmias. *Heart Rhythm* 7 (10), 1438–1445.

- O'Leary, K.A., de Pascual-Teresa, S., Needs, P.W., Bao, Y.P., O'Brien, N.M., Williamson, G., 2004. Effect of flavonoids and vitamin E on cyclooxygenase-2 (COX-2) transcription. *Mutat. Res.* 551 (1–2), 245–254.
- Onai, Y., Suzuki, J., Maejima, Y., Haraguchi, G., Muto, S., Itai, A., Isobe, M., 2007. Inhibition of NF- κ B improves left ventricular remodeling and cardiac dysfunction after myocardial infarction. *American journal of physiology. Am. J. Physiol.* 292 (1), H530–H538.
- Pall, M.L., Levine, S., 2015. Nrf2, a master regulator of detoxification and also antioxidant, anti-inflammatory and other cytoprotective mechanisms, is raised by health promoting factors. *Sheng li xue bao. Acta Psychol. Sin.* 67 (1), 1–18.
- Panchal, S.K., Poudyal, H., Brown, L., 2012. Quercetin ameliorates cardiovascular, hepatic, and metabolic changes in diet-induced metabolic syndrome in rats. *J. Nutr.* 142 (6), 1026–1032.
- Perez, J.R., Higgins-Sochaski, K.A., Maltese, J.Y., Narayanan, R., 1994. Regulation of adhesion and growth of fibrosarcoma cells by NF-kappa B RelA involves transforming growth factor beta. *Cell. Mol. Biol.* 14 (8), 5326–5332.
- Reichert, K., Pereira do Carmo, H. R., Galluce Torina, A., Diógenes de Carvalho, D., Carvalho Sposito, A., de Souza Vilarinho, K. A., da Mota Silveira-Filho, L., Martins de Oliveira, P. P., Petrucci, O., 2016. Atorvastatin Improves Ventricular Remodeling after Myocardial Infarction by Interfering with Collagen Metabolism. *PLoS one.* 11 (11), e0166845.
- Sanders, L.N., Schoenhard, J.A., Saleh, M.A., Mukherjee, A., Ryzhov, S., McMaster Jr, W.G., Nolan, K., Gumina, R.J., Thompson, T.B., Magnuson, M.A., Harrison, D.G., Hatzopoulos, A.K., 2016. BMP antagonist gremlin 2 limits inflammation after myocardial infarction. *Circ. Res.* 119 (3), 434–449.
- Saxena, A., Dobaczewski, M., Rai, V., Haque, Z., Chen, W., Li, N., Frangogiannis, N.G., 2014. Regulatory T cells are recruited in the infarcted mouse myocardium and may modulate fibroblast phenotype and function. *American journal of physiology. Am. J. Physiol.* 307 (8), H1233–H1242.
- Schneiders, D., Heger, J., Best, P., Michael Piper, H., Taimor, G., 2005. SMAD proteins are involved in apoptosis induction in ventricular cardiomyocytes. *Cardiovasc. Res.* 67 (1), 87–96.
- Shahbaz, A.U., Kamalov, G., Zhao, W., Zhao, T., Johnson, P.L., Sun, Y., Bhattacharya, S. K., Ahokas, R.A., Gerling, I.C., Weber, K.T., 2011. Mitochondria-targeted cardioprotection in aldosteronism. *Cardiovasc. Pharmacol.* 57 (1), 37–43.
- Shu, L., Zhang, W., Huang, C., Huang, G., Su, G., 2017. Troxerutin protects against myocardial ischemia/reperfusion injury Via Pi3k/Akt pathway in rats. *Cell Physiol. Biochem.* 44 (5), 1939–1948.
- Spinale, F.G., 2007. Myocardial matrix remodeling and the matrix metalloproteinases: influence on cardiac form and function. *Physiol. Rev.* 87 (4), 1285–1342.
- Sun, Y., 2009. Myocardial repair/remodelling following infarction: roles of local factors. *Cardiovasc. Res.* 81 (3), 482–490.
- Takano-Ishikawa, Y., Goto, M., Yamaki, K., 2006. Structure-activity relations of inhibitory effects of various flavonoids on lipopolysaccharide-induced prostaglandin E2 production in rat peritoneal macrophages: comparison between subclasses of flavonoids. *Phytomedicine. Phytomedicine.* 13 (5), 310–317.
- Tang, J., Lu, L., Liu, Y., Ma, J., Yang, L., Li, L., Guo, H., Yu, S., Ren, J., Bai, H., Yang, J., 2019. Quercetin improve ischemia/reperfusion-induced cardiomyocyte apoptosis in vitro and in vivo study via SIRT1/PGC-1 α signaling. *J. Cell. Biochem.* 120 (6), 9747–9757.
- Urbina, P., Singla, D.K., 2014. BMP-7 attenuates adverse cardiac remodeling mediated through M2 macrophages in prediabetic cardiomyopathy. *American journal of physiology. Am. J. Physiol.* 307 (5), H762–H772.
- Wang, B., Hao, J., Jones, S.C., Yee, M.S., Roth, J.C., Dixon, I.M., 2002. Decreased Smad 7 expression contributes to cardiac fibrosis in the infarcted rat heart. *Am. J. Physiol.* 282 (5), H1685–H1696.
- Wang, L., Tan, A., An, X., Xia, Y., Xie, Y., 2020. Quercetin Dihydrate inhibition of cardiac fibrosis induced by angiotensin II in vivo and in vitro. *Biomed. Pharmacother.* 127, 110205.
- Wei, L.H., Huang, X.R., Zhang, Y., Li, Y.Q., Chen, H.Y., Heuchel, R., Yan, B.P., Yu, C.M., Lan, H.Y., 2013. Deficiency of Smad7 enhances cardiac remodeling induced by angiotensin II infusion in a mouse model of hypertension. *PLoS ONE* 8, (7) e70195.
- Wu, X., Sagave, J., Rutkovskiy, A., Haugen, F., Baysa, A., Nygård, S., Czibik, G., Dahl, C. P., Gullestad, L., Vaage, J., Valen, G., 2014. Expression of bone morphogenetic protein 4 and its receptors in the remodeling heart. *Life Sci.* 97 (2), 145–154.
- Zaafan, M.A., Zaki, H.F., El-Brairy, A.I., Kenawy, S.A., 2013. Protective effects of atorvastatin and quercetin on isoprenaline-induced myocardial infarction in rats. *BFPCC* 51 (1), 35–41.
- Zhang, N., Wei, W.Y., Li, L.L., Hu, C., Tang, Q.Z., 2018. Therapeutic Potential of Polyphenols in Cardiac. *Fibrosis Front. Pharmacol.* 9, 122.